

# Robust bound states in the continuum in Kerr microcavity embedded in photonic crystal waveguide

Evgeny N. Bulgakov and Almas F. Sadreev

*Institute of Physics, Academy of Sciences, 660036 Krasnoyarsk, Russia*

(Dated: April 17, 2014)

We present a two-dimensional photonic crystal design with a microcavity of four defect dielectric rods with eigenfrequencies residing in the propagating band of directional waveguide. In the linear case for tuning of material parameters of defect rods the nonrobust bound state in the continuum (BSC) might occur. The BSC is a result of full destructive interference of resonant monopole and quadrupole modes with the same parity. A robust BSC arises in a self-adaptive way without necessity to tune the parameters of the microcavity with the Kerr effect. Lack of the superposition principle in nonlinear systems gives rise to coupling of the BSC with injecting light. That forms a peculiar shape of isolated transmittance resonance around BSC frequency. We show if injecting light is switched off the BSC stores light that opens a way for light accumulation.

PACS numbers: 42.25.Bs, 42.65.Jx, 03.65.Nk, 42.25.Fx

## I. INTRODUCTION

In 1929, von Neumann and Wigner [1] predicted the existence of discrete solutions of the single-particle Schrödinger equation embedded in the continuum of positive energy states, bound states in the continuum (BSC). Their analysis examined by Stillinger and Herrick [2] long time was regarded as mathematical curiosity because of certain spatially oscillating central symmetric potentials. That situation cardinally changed when Friedrich and Wintgen [3] in framework of two-level Fano-Anderson model formulated the BSC as a resonant state whose width tends to zero as at least one physical parameter varies continuously (see, also [4–7]). Localization of the resonant states of open system, i.e., the BSC can be interpreted as destructive interference of two resonance states which occurs for crossing of eigenlevels of the closed system [7]. That accompanied by avoiding crossing of the resonant states one of which transforms into the trapped state with vanishing width while the second resonant state acquires the maximal resonance width (superradiant state [5, 7]).

The BSC phenomenon is a manifestation of wave interference similar to the Aharonov-Bohm effect or the Anderson localization and is generic in all wave systems. In particular Shipman and Venakides [8] predicted a symmetry protected trapping of electromagnetic waves in periodical array of dielectric rods. Two theoretical groups independently presented examples of the BSC in photonics [9, 10]. In Refs. [9, 11] the infinite periodic double dielectric gratings and two arrays of dielectric cylinders were considered where the BSC is localized in direction cross to the arrays. In Ref. [10] the photonic crystal (PhC) waveguide with directional continuum in two-dimensional PhC of dielectric rods with two off-channel optical microresonators was considered to show various types of the BSC. In both systems the BSC is the result of the Fabry-Perot mechanism for the BSC [12–14] which is accompanied by the Fano resonance collapse in transmittance. In forthcoming papers such photonic BSCs

were experimentally observed [15–18]. A realization of the BSC in the one-dimensional PhC by an advanced digital grading method was described in Ref. [19]. The BSC at surface of half infinite bulk system lays also a new concept for surface states [17, 20–23].

In this letter we present a PhC design of in-channel optical microcavity embedded into the waveguide and show that it capable to realize the BSC as the result of destructive interference of two resonant modes with the same parity decaying into the waveguide continuum. However in the linear open systems the BSC occurs at the unique singular point of space of physical parameters [5, 7, 24] that constitutes a difficulties for experimental visualization of the net BSC in PhC system. First, it is necessary to vary material parameters of the microcavity in order to approach to the BSC point. Second, the BSC is decoupled from the waveguide continuum [7, 24] and therefore the BSC can not be probed by incoming waves.

Our aim is to show that these difficulties can be overcome if to explore the Kerr effect of the optical microcavity. The BSC appears by self-adaptive way due to the Kerr shift of the dielectric constant of the microcavity [25] that transforms the BSC point into the BSC line in the space of frequency and dielectric constant. Also nonlinearity lifts the principle of linear superposition to give rise to that injecting wave interacts with the BSC. Therefore incoming light excites the BSC and forms novel type of complicated response crucially different from Breit-Wigner or Fano type of resonances. Thus the nonlinearity opens a new page in the BSC phenomenon [20, 25] and promises novel nonlinear effects [25, 27–29] in the light transmission.

## II. LINEAR CASE

The layout of photonic crystal (PhC) system is shown in Fig. 1 with parameters given in Figure caption. The single row of the rods is removed from the PhC that forms a directional photonic waveguide which supports a

single band of guided TM mode spanning from the bottom band edge 0.315 to the upper one 0.41 in terms of  $2\pi c/a$  [30]. The TM mode has the electric field component parallel to the infinitely long rods. Four linear defect rods of the same radius with dielectric constant  $\epsilon$  shown by green open circles are placed at vertexes of square. The fifth central defect rod made from the same GaAs material as the ghost rods of PhC is placed in the center of square. These five defect rods form optical microcavity embedded into the PhC waveguide. From both sides of the microcavity additional couple of rods are inserted in the waveguide in order to diminish the coupling constant. The eigenfrequencies of the cavity versus the

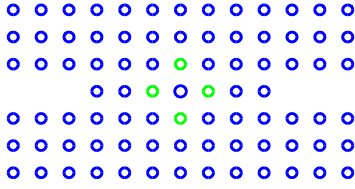


FIG. 1: PhC consists of a square lattice of GaAs rods with linear refractive index  $n_0 = 3.4$  and nonlinear refractive index  $n_2 = 1.5 \times 10^{-13} \text{ cm}^2/\text{W}$  at  $\lambda = 1.55 \text{ m}\mu$  and radius  $0.18a$  in air shown by blue open circles where,  $a$  is the lattice unit. Four linear defect rods of the same radius with dielectric constant  $\epsilon$  are shown by green bold circles.

dielectric constant  $\epsilon$  are plotted in Fig. 2 which are accompanied by the eigenmodes [30]. The quadrupole-xy mode has eigenfrequency beyond the propagation band of PhC waveguide for considered range of interest of  $\epsilon$  in Fig. 2.

The numerical procedure of solution of the Maxwell equations is based on the Lippmann-Schwinger equation

$$[\hat{H}_{eff}(\omega) - \omega^2]\psi_S = \hat{\Gamma}\psi_{in}, \quad (1)$$

where  $\hat{H}_{eff}(\omega)$  is the non-hermitian effective Hamiltonian which is resulted by projection of the total space of the PhC system onto the inner space of the microcavity. Respectively, the scattering function  $\psi_S$  is electric field directed along the rods in the microcavity, while the right-hand expression in Eq. (1) shows as injected light amplitude  $\psi_{in}$  excites the microcavity through the coupling matrix  $\hat{\Gamma}$ . We refer to Refs. [10, 31] for details in application to the PhC. The complex eigenvalues of  $H_{eff}$  have simple physical meaning [32]. Its real parts define resonant frequencies of the cavity, and imaginary parts are responsible for resonance widths. The unique BSC point can be hardly achieved experimentally. Therefore it is important to show by which way to limit to the BSC point in order to reveal the scattering state maximally

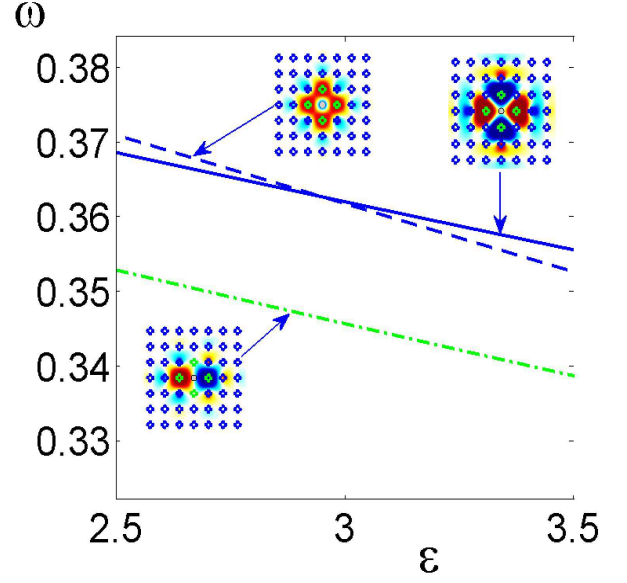


FIG. 2: (Color online) (a) Eigen-frequencies in unit of  $2\pi c/a$  vs dielectric constant of the four defect rods shown by open green circles in Fig. 3. Insets to them show profiles of the eigenmodes.

close to the BSC. In Fig. 3 (a) and (b) we show solutions of Eq. (1) for two frequencies and the dielectric constant of defect rods  $\epsilon = 3.01$ . The first frequency corresponds non resonant transmittance marked by star in Fig. 4 (b) with the corresponding solution shown in Fig. 3 (a). The second choice of frequency corresponds to the resonant transmittance  $|t| = 1$  marked by rhombus in Fig. 4 (b) with the corresponding solution shown in Fig. 3 (b). In Fig. 3 (c) the BSC  $\psi_{BSC}$  is shown which is eigenfunction of the non-hermitian effective Hamiltonian  $H_{eff}(\omega_{BSC})\psi_{BSC} = \omega_{BSC}^2\psi_{BSC}$  with real eigenfrequency  $\omega_{BSC}$  of the BSC. [7, 10, 24]. As seen from Fig. 3 (b) for approaching to the BSC point along the line  $|t| = 1$  reveals the BSC provided that the parameter  $\epsilon$  is close to the BSC point  $\epsilon = 3.004559$ . However the difference between the scattering wave function in Fig. 3 (b) and localized BSC function in Fig. 3 (c) is that the BSC does not support current flows. Fig. 4 (b) shows as the Fano resonance is collapsing for approaching to the BSC magnitude of the dielectric constant.

Numerically, the dimension of the inner space of microcavity takes around of thousands of sites per elementary cell in the finite difference scheme. This numerical routine can be enormously shortened if to use numerically calculated eigenmodes and restrict ourselves by contribution of only two relevant (monopole and quadrupole-diag) eigenmodes. That decimation procedure corresponds to the coupled mode theory (CMT) [33] if to disregard radiation shifts in the effective Hamiltonian. The stationary

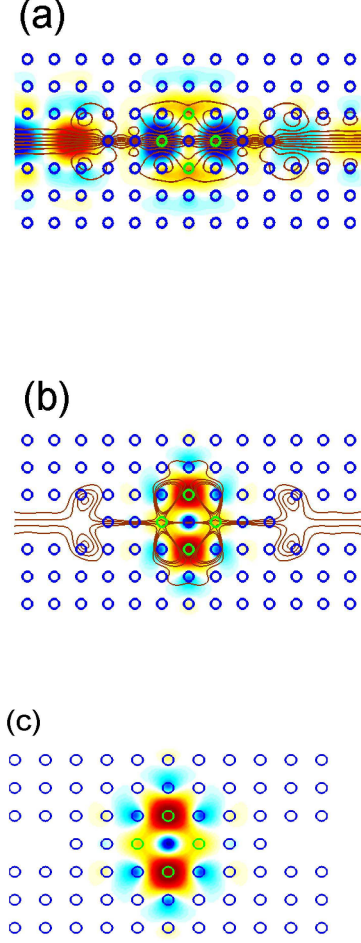


FIG. 3: The solutions of Eq. (1) (real parts) for (a)  $\epsilon = 3.01, \omega = 0.3619$  and (b)  $\epsilon = 3.01, \omega = 0.361755$ . Thin solid line shows current flows. (c) BSC which is the eigenfunction of the effective Hamiltonian in Eq. (1) when its complex eigenvalue becomes real (zero).

CMT equations have the following form

$$[\hat{H}_{eff}^{(2)}(\omega) - \omega] \begin{pmatrix} A_1 \\ A_2 \end{pmatrix} = -i \begin{pmatrix} \sqrt{\gamma_1} \\ \sqrt{\gamma_2} \end{pmatrix} \psi_{in} \quad (2)$$

where

$$\hat{H}_{eff}^{(2)}(\omega) = \begin{pmatrix} \omega_1 - i\gamma_1 & -u - i\sqrt{\gamma_1\gamma_2} \\ -u - i\sqrt{\gamma_1\gamma_2} & \omega_2 - i\gamma_2 \end{pmatrix}, \quad (3)$$

$\psi_{in}$  is the amplitude injected light, the subscripts 1, 2 refer to the monopole and quadrupole-diag eigenmodes. We approximate their eigenfrequencies as follows  $\omega_{1,2} = \omega_0 \pm \Delta$  where the parameters were borrowed from numerics to be equal  $\Delta = 0.0025367(\epsilon - 2.9518)$ ,  $\omega_0 = 0.362443 - 0.01567683(\epsilon - 2.9518)$ . Similar expansions take place if to vary the radius of defect rods. The resonant widths  $\gamma_1, \gamma_2$  were evaluated from transmittance resonances provided that the resonances are not overlapped.

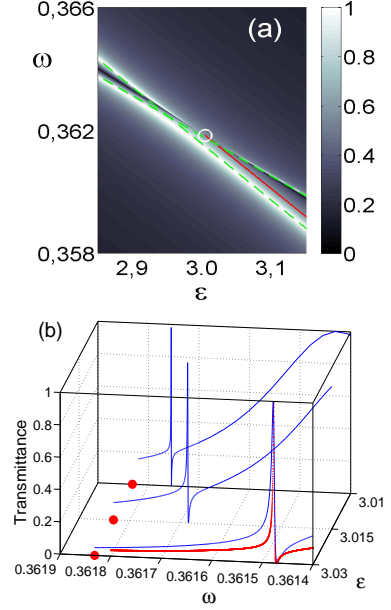


FIG. 4: (Color online) (a) Transmittance vs frequency of injected light and dielectric constant of defect rods in the two-level approximation. The BSC point  $\epsilon = 3.004559, \omega = 0.36183186$  marked by white open circle. It is shown as this BSC point transforms into the line (red) if to take into account the Kerr effect of central defect rod. (b) transmittance vs frequency in the vicinity of the BSC point. The three slice correspond to  $\epsilon = 3.03, 3.015, 3.01$  respectively. Red closed circles mark the BSC frequency. The results of computation for transmittance in PhC are presented by blue line and CMT model by red.

As a result we obtained  $\gamma_1 = 3 \cdot 10^{-5}, \gamma_2 = 1.3 \cdot 10^{-4}$ . The coupling constant between the modes  $u$  was evaluated by fitting of the BSC point in the CMT approach to the BSC point evaluated in numerical solution of the Maxwell equations based on Eq. (1) to obtain  $u = 1.768583 \cdot 10^{-4}$ . The amplitude of transmittance is given by expression [33]

$$t = \psi_{in} + \sqrt{\gamma_1} A_1 + \sqrt{\gamma_2} A_2 \quad (4)$$

Comparison of the CMT approximation with numerical solution of full equation (1) demonstrates good agreement. For CMT approach the BSC point can be found analytically from equation  $\text{Det}[\hat{H}_{eff}^{(2)} - \omega] = 0$  which equals [5, 7]

$$\omega_2 - \omega_1 = \frac{u(\gamma_2 - \gamma_1)}{\sqrt{\gamma_1\gamma_2}}, \omega_{BSC} = \omega_2 + u\sqrt{\frac{\gamma_2}{\gamma_1}}. \quad (5)$$

Among many intriguing properties of the BSC it's point is singular in parametric space of  $\omega$  and  $\epsilon$  [7, 11, 24]. The transmittance and scattering wave function crucially depend on a way in the space  $\omega, \epsilon$  to limit to the BSC point in the vicinity of radius about the coupling strengths. A feature of light transmittance shown in Fig. 4 is that

line of zero transmittance touches of unit transmittance at the BSC point shown in Fig. 4 by white open circle [5, 7, 15].

### III. NONLINEAR CASE

Above consideration for the linear case shows that revelation of the BSC demands fine tuning of material parameter (dielectric constant or diameter) of defect rods in order to satisfy equation for the BSC point (5). Therefore a probing of BSC features in light transmittance by injecting light of monochromatic laser is a challenge for experiment. We show that account of the Kerr effect can lift this problem making the BSC point self adaptive without a tuning of material parameters of the defect rods [25, 26].

In the vicinity of the BSC point light intensity is sufficiently large only in the microcavity. Therefore it is enough to modify the effective Hamiltonian  $\hat{H}_{eff}^{(2)} \rightarrow \hat{H}_{eff}^{(2)} + \hat{V}$ . The matrix elements of perturbation  $\hat{V}$  in the two-level approximation equal [34]

$$V_{mn} = -\frac{(\omega_m + \omega_n)}{4N_m} \int d^2\vec{r} \delta\epsilon(\vec{r}) E_m(\vec{r}) E_n(\vec{r}), m, n = 1, 2, \quad (6)$$

where  $E_m(\vec{r})$  are the eigenmodes of the linear microcavity shown in Fig. 2 with normalization [35]

$$N_m = \int d^2\vec{r} \epsilon_{PhC} E_m^2(\vec{r}) = \frac{a^2}{cn_2}, \quad (7)$$

$\epsilon_{PhC}$  is the dielectric constant of whole defectless PhC.

$$\delta\epsilon(\vec{r}) = \frac{n_0 cn_2 |E(\vec{r})|^2}{4\pi} \approx \frac{n_0 cn_2 |\sum_m A_m E_m(\vec{r})|^2}{4\pi} \quad (8)$$

is the nonlinear contribution to the dielectric constant of the defect rod with instantaneous Kerr nonlinearity. After substitution of matrix (6) into the CMT equation (2) we obtain the nonlinear system of equations for the mode amplitudes  $A_m$ .

Two factors substantially weakens the nonlinear contribution into the quadrupole-diag mode. First, as seen from Fig. 2 two nodal lines of the quadrupole mode go through the central defect rod. Second,  $\gamma_1 \ll \gamma_2$  to give rise to inequality  $\lambda_{11} I_1 \ll \lambda_{22} I_2$  where [31]

$$\lambda_{mn} = \frac{c^2 n_2^2}{a^2} \int E_m^2(x, y) E_n^2(x, y) d^2\vec{r}. \quad (9)$$

Therefore we can restrict ourselves by the nonlinear shift of the first monopole mode frequency  $\omega_1 \rightarrow \omega_1 + V_{11} = \omega_1 - \lambda_{11} |A_1|^2$  only. Then Eq. (5) gives that the BSC point is achieved if the intensity of the monopole excitement equals

$$\lambda_{11} I_{1c} = \lambda_{11} |A_1|^2 = \omega_2 - \omega_1 - \frac{u(\gamma_2 - \gamma_1)}{\sqrt{\gamma_1 \gamma_2}}, \quad (10)$$

with the BSC frequency defined in Eq. (5). From equation for the BSC  $\text{Det}[\hat{H}_{eff}^{(2)}] = 0$  and second equation in CMT equations (2) we have an equality  $(\omega_{BSC} - \omega_2 + i\gamma_2) A_2 + (u + i\sqrt{\gamma_1 \gamma_2}) A_1 = 0$  which defines the intensity of the quadrupole-diag mode at the BSC point

$$I_{2c} = |A_{2c}|^2 = \frac{\gamma_1}{\gamma_2} I_{1c}. \quad (11)$$

Both BSC intensities are marked in Fig. 5 (a) by open circles.

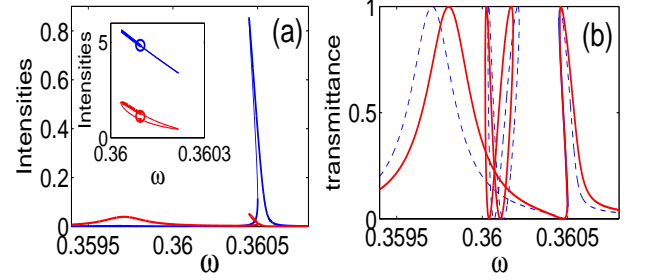


FIG. 5: (Color online) (a) Intensities of excitation of the monopole mode  $|A_1|^2$  (blue lines) and quadrupole mode  $|A_2|^2$  (red lines). The basic window shows the first family which inherits the linear case and inset shows the BSC family. Thin lines response for unstable solutions and thicker lines show stable solutions. (b) Transmittance vs frequency of injected light with the amplitude  $\psi_{in} = 0.0025$  with account of Kerr effect with  $\lambda_{11} = 0.0001$ . The dielectric constant of vertex rods  $\epsilon = 3.1$ . Transmittance calculated from the nonlinear CMT equations (2) is shown by blue dash line and transmittance calculated from the nonlinear Maxwell equations is shown by red solid line.

After substitution of the nonlinear term  $\omega_1 \rightarrow \omega_1 - \lambda_{11} |A_1|^2$  into Eq. (2) and solving of self-consistent nonlinear equations we obtain two different families of the solutions [25]. The first family of solutions inherits the linear case and for small injecting power has typical resonance behavior for the mode intensities  $|A_1|^2, |A_2|^2$  shown in Fig. 5 (a) in basic window. Those mode (monopole) which has smaller resonant width undergoes larger excitation and larger typical decline to the left because of negative contribution of the nonlinear term to the first monopole mode. The second BSC family of solutions are loops centered at the BSC point (10) shown in inset of Fig. 5 (a). A stability of the solutions are notified by thicker lines. When the amplitude of injecting light  $\psi_{in}$  tends to zero the size of loops is shrinking to the BSC points marked by open circles. The transmittance calculated by Eq. (4) is plotted in Fig. 5 (b) for both families and clearly reflects the frequency behavior in Fig. 5 (a). The transmittance on the basis of full range nonlinear Maxwell equations is plotted in Fig. 5 (b) by solid red line to demonstrate good agreement. The BSC solutions exist for a whole range of linear diffractive index as plotted by red line in Fig. 4 (a) that indeed makes the BSC for nonlinear optical microcavity flexible relative to choice of material parameter. By the terminology



proposed in Ref. [8] we call such a BSC as the robust BSC.

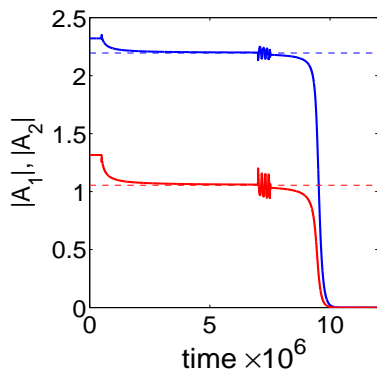


FIG. 6: (Color online) Time evolution of mode amplitudes after the injecting light with amplitude power  $\psi_{in} = 0.0025$  was switched off at time  $0.5 \times 10^6$  and then light impulse of duration  $0.5 \times 10^6$  was applied at the time  $7 \times 10^6$ . Dash lines show the BSC amplitudes given by Eqs. (10) and (11).

One can see from Fig. 5 (a) that intensities of mode excitation at the BSC solution substantially exceed the intensities for the solution inherited the linear case, at least, for small injecting amplitudes. The values  $I_{1c}, I_{2c}$  around which the intensities are centered can be enhanced by increasing of the linear refractive index of four defect rods or by decreasing of the nonlinear refractive index of the central defect rod as Eqs. (10) and (11) show. That prompts to use the BSC solution for storage of light. Indeed, Fig. 6 shows time evolution of the mode amplitudes after injecting light was switched off. The amplitudes fastly evolve from current values to the BSC values given by Eq. (10) and shown by dash lines in Fig. 6. Also it is easy to release this accumulated energy by short impulse of light injected into the PhC waveguide. These results open a way for light energy accumulation and release.

**Acknowledgments.** The paper was partially supported by RFBR grant 13-02-00497 and grant of RSCF 14-12-00266. We acknowledge discussions with Chia Wei Hsu and D.N. Maksimov.

- 
- [1] J. von Neumann and E. Wigner, Phys. Z. **30**, 465 (1929).
  - [2] F.H. Stillinger and D.R. Herrick, Phys. Rev. A **11**, 446 (1975).
  - [3] H. Friedrich and D. Wintgen, Phys. Rev. A **32**, 3231 (1985).
  - [4] T.V. Shahbazyan and M.E. Raikh, Phys. Rev. B **49**, 17123 (1994).
  - [5] A. Volya and V. Zelevinsky, Phys. Rev. C **67**, 054322 (2003).
  - [6] M. L. Ladrón de Guevara, F. Claro, and P. A. Orellana, Phys. Rev. B **67**, 195335 (2003).
  - [7] A.F. Sadreev, E.N. Bulgakov, and I. Rotter, Phys. Rev. B **73**, 235342 (2006).
  - [8] S.P. Shipman and S. Venakides, Phys. Rev. E **71**, 026611 (2005).
  - [9] D. C. Marinica, A. G. Borisov, and S.V. Shabanov, Phys. Rev. Lett. **100**, 183902 (2008).
  - [10] E.N. Bulgakov and A.F. Sadreev, Phys. Rev. B **78**, 075105 (2008).
  - [11] R.F. Ndagali and S.V. Shabanov, J. Math. Phys. **51**, 102901 (2010).
  - [12] C.S. Kim, A.M. Satanin, Y.S. Joe, and R.M. Cosby, Phys. Rev. B **60**, 10962 (1999).
  - [13] Shanhui Fan *et al*, Phys. Rev. B **59**, 15882 (1999).
  - [14] I. Rotter and A.F. Sadreev, Phys. Rev. E **69**, 066201 (2004); *ibid* **71**, 046204 (2005).
  - [15] T. Lepetit, E. Akmansoy, J.-P. Ganne, and J.-M. Lourtioz, Phys. Rev. B **82**, 195307 (2010).
  - [16] Y. Plotnik, *et al*, Phys. Rev. Lett. **107**, 183901 (2011).
  - [17] G. Corrielli, G. Della Valle, A. Crespi, R. Osellame, and S. Longhi, Phys. Rev. Lett. **111**, 220403 (2013).
  - [18] Chia Wei Hsu, *et al*, Nature, 499, 188 (2013).
  - [19] N. Prodanovic, V. Milanovic, and J. Radovanovic, J. Phys. A: Math. Gen **42**, 415304 (2009).
  - [20] M.I. Molina, A.E. Miroshnichenko, and Yu.S. Kivshar, Phys. Rev. Lett. **108**, 070401 (2012).
  - [21] Chia Wei Hsu, *et al*, Light: Science and Applications **2**, 1 (2013).
  - [22] S. Weimann *et al*, Phys. Rev. Lett. **111**, 240403 (2013).
  - [23] N.A. Gallo and M.I. Molina, cond-mat. arXiv:1401.7380v1 (2014).
  - [24] E.N. Bulgakov, K.N. Pichugin, A.F. Sadreev, and I. Rotter, JETP Lett. **84**, 508 (2006).
  - [25] E.N. Bulgakov and A.F. Sadreev, Phys. Rev. B **80**, 115308 (2009); *ibid* **81**, 115128 (2010).
  - [26] G. Della Valle and S. Longhi, Phys. Rev. B **89**, 115118 (2014).
  - [27] S.P. Shipman, J. Ribbeck, K.H. Smith, and C. Weeks, IEEE Photonics J. **2**, 911 (2010).
  - [28] R.F. Ndagali and S.V. Shabanov, Proc. of SPIE **8808**, (2013).
  - [29] E.N. Bulgakov and A.F. Sadreev, J. Opt. Soc. Am. B **30**, 2549 (2013).
  - [30] K. Busch, S.F. Mingaleev, A. Garcia-Martin, M. Schillinger, and D. Hermann, J. Phys. : Cond. Mat. **15**, R1233 (2003).
  - [31] E.N. Bulgakov and A.F. Sadreev, Phys. Rev. B **86**, 075125 (2012).
  - [32] J. Okołowicz, M. Płoszajczak, and I. Rotter, Phys. Rep. **374**, 271 (2003).
  - [33] C. Manolatou *et al*, IEEE J. Quantum Electron. **35**, 1322 (1999).
  - [34] E. Bulgakov, K. Pichugin, and A. Sadreev, Phys. Rev. B **83**, 045109 (2011).
  - [35] M. Soljačić, C. Luo, J. D. Joannopoulos, and S. Fan, Opt. Lett. **28**, 637 (2003).